JOURNAL OF SOLID STATE CHEMISTRY 112, 329–339 (1994)

^{51}V NMR Studies of Crystalline Monovalent and Divalent Metal Metavanadates

Satoshi Hayakawa, Toshinobu Yoko,[1] and Sumio Sakka

Institute for Chemical Research, Kyoto University, Uji, Kyoto-fu 611, Japan

Received August 31, 1993; in revised form December 13, 1993; accepted December 16, 1993

^{51}V static and magic-angle spinning (MAS) NMR spectra of crystalline monovalent metal metavanadates $LiVO_3$, α- and β-$NaVO_3$, KVO_3, $CsVO_3$, β-$AgVO_3$, and NH_4VO_3 and divalent metal metavanadates $M(VO_3)_2$ (M = Mg, Ca, Sr, Ba, Zn, Pb) have been measured in order to establish the relationships between the various NMR parameters, such as isotropic chemical shift, δ_{iso}, chemical shift anisotropy, $|\Delta\delta|$, the asymmetry parameter, η, and the crystallographic parameters. When the structural units are the same, in this case VO_4 tetrahedra or VO_5 trigonal bipyramids, the δ_{iso} decrease almost linearly with decreasing average V–O bond length, independent of the polymerization degree and linkage mode of the VO_n polyhedra. $|\Delta\delta|$ increases with the polymerization degree and the degree of the structural distortion of the VO_n polyhedron. It is found possible to predict the structural unit and the polymerization degree on the basis of the relation between $|\Delta\delta|$ and η.

INTRODUCTION

In our previous paper (1), we performed extensive studies on the local structure around V^{5+} in various divalent metal ortho- and pyrovanadate crystals by means of ^{51}V static and MAS NMR. For crystalline orthovanadates consisting of isolated VO_4 tetrahedra, the ^{51}V isotropic chemical shift, δ_{iso}, decreases linearly with decreasing electronegativity (EN) of divalent metals surrounding the VO_4 unit. The small differences in the structural distortion of VO_4 units and the oxygen coordination number of the divalent cation do not influence their correlation. This indicates that the magnetic shielding of vanadium in the divalent metal orthovanadates is largely dependent on the electron density of four oxygens surrounding V^{5+} tetrahedrally, which in turn is determined by the EN of the divalent metal, i.e., its electron-donating ability.

A similar linear relationship between δ_{iso} and EN was observed for the divalent metal pyrovanadates of dichromate-type. In this case, however, the slope of the linear plot for pyrovanadates was about one-half that for orthovanadates. Such a difference was explained as follows. The tetrahedral VO_4 unit in orthovanadates is isolated and surrounded solely by divalent cations, while in pyrovanadates two tetrahedral VO_4 units are linked together by sharing their corners to form a V_2O_7 unit, leading to a decrease in the number of divalent cations surrounding a VO_4 unit. From this point of view, it is of interest to investigate the effects of the EN of different metals on the ^{51}V chemical shift in various metavanadates which consist of $(VO_3)_n$ single chains or $(V_2O_8)_n$ double zigzag chains.

Mastikhin *et al.* (2) have measured the ^{51}V static NMR spectra of various crystalline alkali vanadates and determined the chemical shift tensors, δ_1, δ_2, and δ_3. It was shown that in alkali metavanadates the chemical shift anisotropy, $\delta_1-\delta_3$, increases with increasing structural distortion of the VO_4 tetrahedron. Eckert and Wachs (3) have determined the isotropic chemical shift of crystalline vanadates by ^{51}V static and magic-angle spinning (MAS) NMR methods in two different magnetic fields, 7.05 and 11.7 T, and have made a correction for the second-order quadrupolar shift of it. Hayashi *et al.* (4) have also measured the ^{51}V static and MAS NMR spectra of crystalline alkali and ammonium metavanadates and discussed the correlation of the isotropic chemical shifts and the chemical shift anisotropies with the structural parameters, such as average V–O bond length, average M–O bond length, the O–V–O bond angle, and oxygen coordination numbers around the vanadium and alkali metals, M. However, since all those studies dealt mainly with crystalline metavanadates containing monovalent cations, the relationship between the ^{51}V NMR parameters and the local structural environment around the vanadium atoms has not been well established for all crystalline metavanadates.

In the present paper, the ^{51}V static and MAS NMR spectra are systematically measured for a large number of crystalline monovalent (Li, Na, K, Cs, Ag, NH_4) and divalent (Mg, Ca, Sr, Ba, Zn, Pb) cation metavanadates with known crystal structures to determine the isotropic chemical shift, the chemical shift anisotropy, and the asymmetry parameter. On the basis of the present mea-

[1] To whom correspondence should be addressed.

0022-4596/94 $6.00

TABLE 1
Conditions for Synthesis of Crystalline Metavanadates

Crystal	Starting materials		Temperature (°C) time (hr)	JCPDS-FILE and refs.
$Zn_3(VO_4)_2$	ZnO,	V_2O_5	780/72	19-1469 (17)
$LiVO_3$	Li_2CO_3,	V_2O_5	900(m)[a] → Tr[b]	33-835 (19)
α-$NaVO_3$	β-$NaVO_3$		450/24	32-1197 (8)
KVO_3	K_2CO_3,	V_2O_5	900(m) → Tr	33-1052 (10)
$CsVO_3$	Cs_2CO_3,	V_2O_5	600/48	37-165
β-$AgVO_3$	$AgNO_3$,	V_2O_5	390/96	29-1154 (18)
$Mg(VO_3)_2$	MgO,	V_2O_5	750/48	34-13 (11)
$Ca(VO_3)_2$	$CaCO_3$,	V_2O_5	770/24	23-137 (12)
$Sr(VO_3)_2$	$SrCO_3$,	V_2O_5	620/24	29-1318
$Ba(VO_3)_2$	$BaCO_3$,	V_2O_5	900(m) → 650/48	26-204 (14)
$Zn(VO_3)_2$	ZnO,	V_2O_5	600/48	23-757 (13)
$Pb(VO_3)_2$	PbO,	V_2O_5	600(m) → 460/24	29-789 (16)

[a] Melting temperature.
[b] Room temperature.

surements for metavanadates and the previous ones for ortho- and pyrovanadates (1), relationships between the crystallographic parameters and the ^{51}V NMR parameters of various crystalline vanadates have been fully examined.

EXPERIMENTAL

Sample Preparation

Crystalline vanadates studied were monovalent metal metavanadates $LiVO_3$, α- and β-$NaVO_3$, KVO_3, $CsVO_3$, β-$AgVO_3$, and NH_4VO_3 and divalent metal metavanadates $M(VO_3)_2$ (M = Mg, Ca, Sr, Ba, Zn, and Pb). β-$NaVO_3$ and NH_4VO_3 were obtained from Nacalai Tesque Co., Ltd. Other crystalline metavanadates were prepared from the reagent-grade chemicals, V_2O_5, Li_2CO_3, K_2CO_3, Cs_2CO_3, $AgNO_3$, MgO, $CaCO_3$, $SrCO_3$, $BaCO_3$, ZnO, and PbO, supplied by Nacalai Tesque and Wako Chemicals Co., Ltd. Crystals of $LiVO_3$, KVO_3, $Ba(VO_3)_2$, and $Pb(VO_3)_2$ were synthesized by crystallization from the melts. Other crystals were synthesized by solid-state reaction of the starting powder mixture. Conditions for synthesis of all the crystalline vanadates are shown in Table 1. The crystalline phases of all the samples were identified by comparing their powder X-ray diffraction patterns with the data of JCPDS-FILE.

NMR Measurements

^{51}V static and MAS NMR spectra of powdered crystalline vanadates were recorded at 105 MHz (9.4 T) on a JEOL JNM-GSX400MAS FT-NMR spectrometer. A single pulse sequence was used: a pulse length of 0.5–2.0 μsec corresponding to a pulse angle of ~22.5°, a pulse delay of 1 sec, and the accumulation of 400–1000 scans. A cylindrical zirconia rotor was rotated at a speed of about 6 kHz in the ^{51}V MAS NMR measurements. The ^{51}V MAS NMR spectra were obtained at two sample spinning speeds in the range 4–6 kHz to differentiate the main peak from spinning side bands. The isotropic chemical shifts were determined from the position of the main peak, which did not change with the sample spinning speed. The ^{51}V NMR chemical shift is expressed in terms of the δ scale with respect to $Zn_3(VO_4)_2$ used as the second external reference, which is assumed to have $\delta = -522$ ppm (3). Accordingly, the ^{51}V NMR chemical shifts are presented with reference to $VOCl_3$ neat liquid, which is assumed to have $\delta = 0$ ppm. The right-hand side of the horizontal axis corresponds to the lower resonance frequency (high magnetic field).

Generally line broadening is caused by chemical shift anisotropy, dipole–dipole interaction, and quadrupolar interaction in the static NMR spectra. The use of higher magnetic field increases the chemical shift anisotropy but decreases the quadrupolar interaction (5). The broadening due to chemical shift anisotropy gives a typical powder pattern arising from an isotropic distribution of the direction of principal axes of the chemical shift tensor with respect to the external magnetic field (6, 22). The principal components of the chemical shift tensor, δ_1, δ_2, and δ_3, were determined from the positions of the peak and shoulder of the ^{51}V static NMR spectra as shown later (Fig. 2). The chemical shift anisotropy, $\Delta\delta$, and asymmetry parameter, η, were determined by using the definitions (4, 7)

$$\Delta\delta = \delta_3 - \frac{\delta_1 + \delta_2}{2} \qquad [1]$$

TABLE 2
Local Symmetry of VO_4 Tetrahedra and VO_5 Trigonal Bipyramids, Average V–O Bond Length, V–O–V Bond Angle, and Average Angle of Twist in Monovalent and Divalent Metal Metavanadates Calculated from Reference Data (8–19)

Compound	Structural unit	Local point symmetry	Site No.	Average V–O bond length (Å)	Δd_n (10^{-2} Å)	Δa_n (degrees)	V–O–V bond angle (degrees)	Average angle of twist (degrees)
				Divalent metal metavanadate				
$Mg(VO_3)_2$	VO_5	Cs	—	1.83	13	13.8	—	—
$Ca(VO_3)_2$	VO_5	Cs	—	1.82	13	16.8	—	—
$Sr(VO_3)_2$	VO_4	—	—	—	—	—	—	—
$Ba(VO_3)_2$	VO_4	E	1	1.79	10	9.8	156	52(15)[a]
	VO_4	C_2	2	1.78	6	9.8	160	11(11)
$Zn(VO_3)_2$	VO_5	E	—	1.84	12	11.4	—	—
$Pb(VO_3)_2$	VO_5	Cs	1	1.84	14	17.2	—	—
	VO_5	Cs	2	1.85	15	17.5	—	—
				Monovalent metal metavanadate				
$LiVO_3$	VO_4	E	—	1.72	8	2.7	140.6	4(3)
α-$NaVO_3$	VO_4	E	—	1.73	8	1.7	135.6	5(1)
β-$NaVO_3$	VO_5	Cs	—	1.83	13	17.4	—	—
KVO_3	VO_4	Cs	—	1.73	11	1.8	143	8.5(4)
$CsVO_3$	VO_4	—	—	—	—	—	—	—
β-$AgVO_3$	—	—	—	—	—	—	—	—
NH_4VO_3	VO_4	Cs	—	1.73	7	1.5	145	3(1)
V_2O_5	VO_5	Cs	—	1.82	13	16.8	—	—

[a] The values within the parentheses are estimated standard deviations.

$$\eta = \frac{\delta_2 - \delta_1}{\delta_3 - \delta_{iso(static)}} \quad [2]$$

$$\delta_{iso(static)} = \frac{\delta_1 + \delta_2 + \delta_3}{3}, \quad [3]$$

where $\delta_{iso(static)}$ is the isotropic chemical shift determined from ^{51}V static NMR. The principal components of the chemical shift tensor were determined based on the following equation (4):

$$|\delta_3 - \delta_{iso(static)}| \geq |\delta_1 - \delta_{iso(static)}| \geq |\delta_2 - \delta_{iso(static)}|. \quad [4]$$

The asymmetry parameter, η, is a measure of the deviation of chemical shift tensors from axial symmetry; $\eta = 0$ for axially symmetric electron distribution around a vanadium atom and $\eta = 1$ for nonaxially symmetric electron distribution.

RESULTS

All crystalline vanadates prepared in this study showed X-ray powder diffraction patterns identical to the data in the JCPDS-FILE as shown in the last column of Table 1. No extra peaks were found for each sample, showing that it consisted of a single phase.

Table 2 lists the structural units and crystallographic parameters of the crystalline metavanadates, such as average V–O bond length (<2.2 Å), V–O–V bond angle, and average angle of twist about the V–V axis calculated from the crystallographic data (8–19). The point symmetries of VO_4-tetrahedra and VO_5 trigonal bipyramids are expressed by Schoenflies symbols. The degree of the structural distortion of VO_4 tetrahedra and VO_5 trigonal bipyramids is expressed by the following two parameters (1):

For VO_4 tetrahedra

$$\Delta d_n = \Sigma|(V\text{–}O)_d - \overline{(V\text{–}O)}_d|/4 \quad [5]$$

$$\Delta a_n = \Sigma|(O\text{–}V\text{–}O)_a - \overline{(O\text{–}V\text{–}O)}_a|/6. \quad [6]$$

For VO_5 trigonal bipyramids,

$$\Delta d_n = \Sigma|(V\text{–}O)_d - \overline{(V\text{–}O)}_d|/5 \quad [7]$$

$$\Delta a_n = \Sigma|(O\text{–}V\text{–}O)_a - \overline{(O\text{–}V\text{–}O)}_a|/10, \quad [8]$$

where $(V\text{–}O)_d$ is the V–O bond length, $\overline{(V\text{–}O)}_d$ is the average V–O bond length, $(O\text{–}V\text{–}O)_a$ is the O–V–O bond angle, and $\overline{(O\text{–}V\text{–}O)}_a$ is the average O–V–O bond

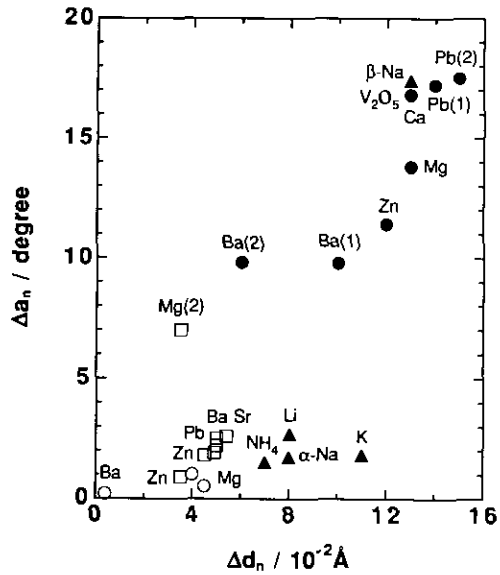

FIG. 1. Plots of Δd_n vs Δa_n. The numbers in the parentheses are the vanadium site numbers. Orthovanadates, ○; pyrovanadates, □; metavanadates, MVO_3, ▲, $M(VO_3)_2$, ●.

angle. In Fig. 1 Δa_n is plotted against Δd_n. For comparison, the data of ortho- and pyrovanadates examined previously (1) are also shown. It appears that Δa_n increases with increasing Δd_n, indicating that these two parameters are well correlated with the structural distortion of the VO_4 tetrahedron and the VO_5-trigonal bipyramid.

Figure 2 shows the ^{51}V static NMR spectra of crystalline monovalent metavanadates: $LiVO_3$, α- and β-$NaVO_3$, KVO_3, $CsVO_3$, β-$AgVO_3$, and NH_4VO_3. The lineshapes of these spectra are very similar to each other except for β-$NaVO_3$ and β-$AgVO_3$. Figure 3 shows the ^{51}V MAS NMR spectra of crystalline monovalent metavanadates, which in all cases consist of a unique isotropic chemical shift denoted by an asterisk and a number of spinning sidebands (SSB). It is seen that the isotropic chemical shifts change with the kind of the monovalent metal cation. Since the ^{23}Na nucleus ($I = 3/2$), which is a quadrupolar nucleus subjected not only to magnetic field but also to electric field gradients, has a resonance frequency at 105.74 MHz, the ^{23}Na NMR signal was observed near the resonance frequency of the ^{51}V nucleus (105.07 MHz), as indicated by a cross in Figs. 2 and 3. Accordingly, the spectra of α- and β-$NaVO_3$ consist of both ^{51}V and ^{23}Na NMR signals.

Figure 4 shows the ^{51}V static spectra of crystalline divalent metal metavanadates $M(VO_3)_2$ (M-Mg, Ca, Sr, Ba, Zn, Pb) and V_2O_5. These spectra are classified into two groups according to the lineshape and linewidth: the first group contains V_2O_5 and $M(VO_3)_2$ (M = Mg, Ca, Zn, Pb), and the second group $Sr(VO_3)_2$ and $Ba(VO_3)_2$. The spectra of the first group are characterized by a sharp peak at high frequency and a long tail extending up to low frequency. It is interesting to note that the spectra of β-$NaVO_3$ and β-$AgVO_3$ in Fig. 2 belong to the first group. On the other hand, the spectra of the second group, which have a narrow linewidth compared with the first group, are very similar in shape to those of monovalent cation metavanadate except β-$NaVO_3$ and β-$AgVO_3$. Figure 5 shows the ^{51}V MAS NMR spectra of crystalline divalent metavanadates, which also in all cases consist of a unique isotropic chemical shift denoted by an asterisk and a number of SSB. It is also seen that the isotropic chemical shifts depend on the kind of the divalent metal cation.

Table 3 summarizes the chemical shift tensor values of δ_1, δ_2, and δ_3, the chemical shift anisotropy, $|\Delta\delta|$, and the

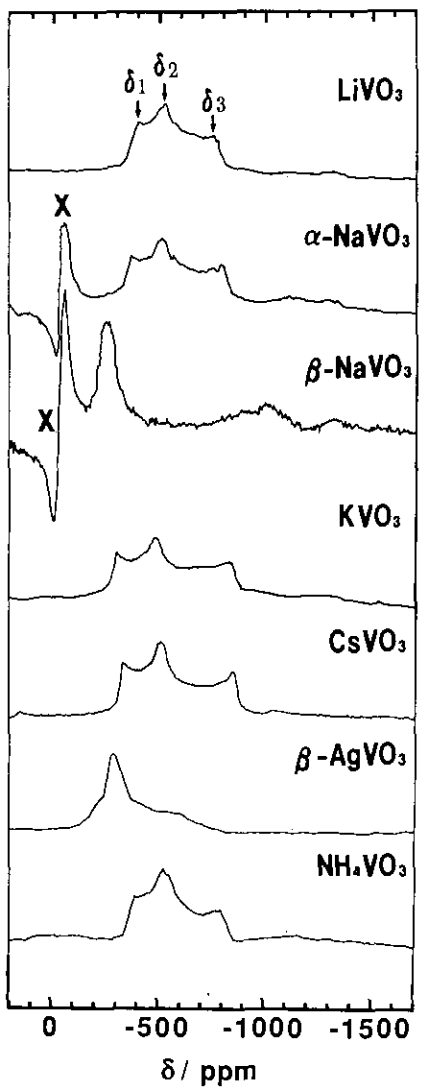

FIG. 2. ^{51}V static NMR spectra of various crystalline monovalent metal metavanadates.

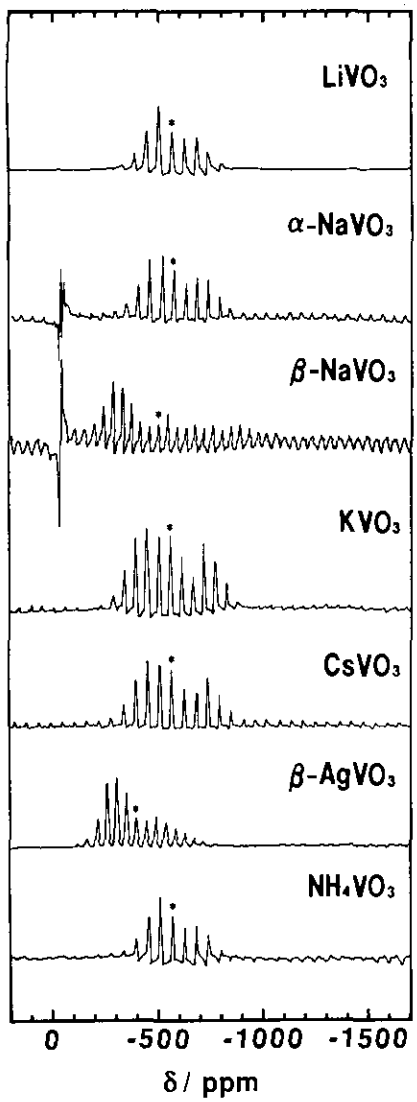

FIG. 3. ^{51}V MAS NMR spectra of various crystalline monovalent metal metavanadates. Isotropic chemical shifts are indicated by asterisks.

asymmetry parameter, η, obtained for several crystalline metavanadates. For comparison, the isotropic chemical shifts of metavanadates ($Zn(VO_3)_2$, $Pb(VO_3)_2$), monovalent metavanadates, and V_2O_5 taken from Refs. (3, 4) are also shown in Table 3. The difference between the isotropic chemical shifts determined from MAS NMR and those from the static NMR method is less than 17 ppm, which is within the full-width at half-maximum (FWHM) of about 20 ppm obtained from the main peak of the MAS NMR spectrum. In addition, the difference in isotropic chemical shift between the present and the reference data (3, 4) is less than 5 ppm except for $Zn(VO_3)_2$. The agreement is excellent and the second quadrupolar shifts are estimated to be less than -7 ppm (3), which is also within the experimental errors (ca. 20 ppm). Therefore, no correction for second-order quadrupolar shift was made in the present study. The differences in chemical shift anisotropies and asymmetry parameters between the present and the reference data (4) are less than 13 ppm and 0.1, respectively, which both are within the experimental errors.

DISCUSSION

The ^{51}V Isotropic Chemical Shifts

Crystalline metavanadates having crystallographically inequivalent vanadium sites should exhibit the same number of ^{51}V isotropic chemical shifts as the sites, as was observed for some ortho- and pyrovanadates (1). As can

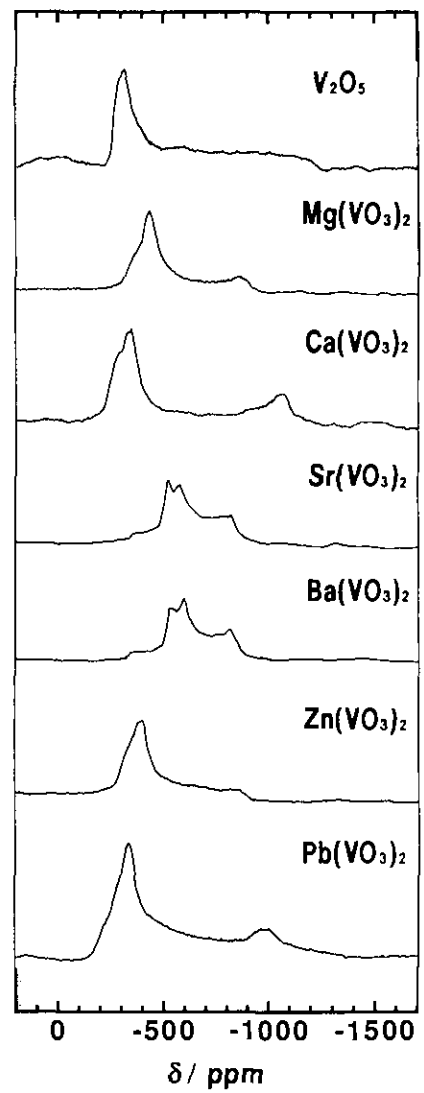

FIG. 4. ^{51}V static NMR spectra of various crystalline divalent metal metavanadates.

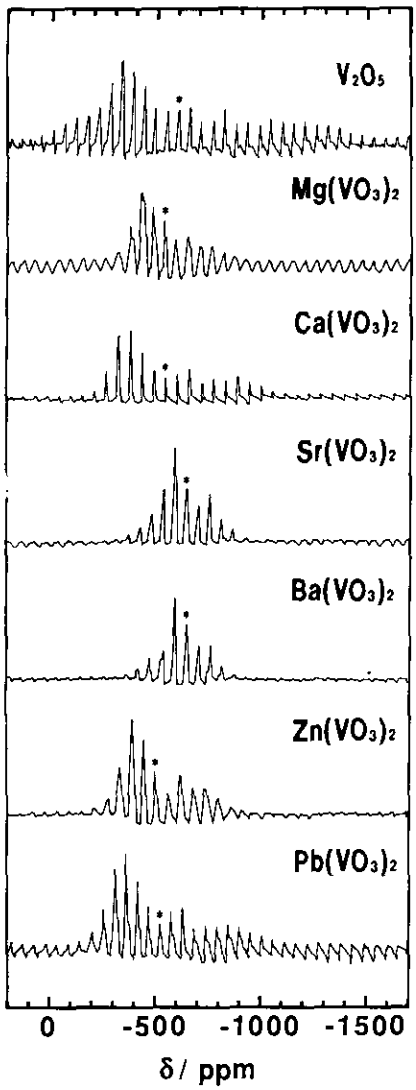

FIG. 5. ^{51}V MAS NMR spectra of various crystalline divalent metal metavanadates. Isotropic chemical shifts are indicated by asterisks.

be seen in Table 2, in $Ba(VO_3)_2$ and $Pb(VO_3)_2$ there are two crystallographically inequivalent vanadium sites. Both crystals, however, exhibit only one isotropic chemical shift, probably due to those vanadium sites being magnetically equivalent within the experimental resolution of the spectrum of 0.5 ppm. Other metavanadates, in which every vanadium is crystallographically equivalent, showed a unique isotropic chemical shift as expected.

In ortho- and pyrovanadates the ^{51}V isotropic chemical shifts determined from ^{51}V MAS NMR were found to be very sensitive to the electronegativity of the second neighboring cations, M, through the variation of the electron density in the VO_4 tetrahedron (1). In Fig. 6 the ^{51}V isotropic chemical shifts, δ_{iso}, of various crystalline metavanadates determined by ^{51}V MAS NMR are plotted against Pauling's EN of the monovalent and divalent metal atom, M. For comparison, the data of ortho- and pyrovanadates studied previously (1) are also shown by a solid line with open circles and a dotted line with open squares, respectively. In monovalent metal metavanadates, denoted by solid triangles, the isotropic chemical shift decreases in the order β-$AgVO_3$ > β-$NaVO_3$ > KVO_3 > $LiVO_3$ ~ α-$NaVO_3$ > $CsVO_3$, and does not correspond to the decreasing order of the electronegativity of the monovalent metal atom: Ag > Li > Na > K > Cs. In divalent metal metavanadates denoted by solid circles the isotropic chemical shift decreases in the order $Zn(VO_3)_2$ > $Pb(VO_3)_2$ > $Mg(VO_3)_2$ > $Ca(VO_3)_2$ > $Sr(VO_3)_2$ > $Ba(VO_3)_2$, while the electronegativity of the divalent metal atom decreases in the order Pb > Zn > Mg > Ca > Sr > Ba. In addition, it is difficult to draw a unique straight line going through the data points of metavanadates due to large scattering, although there seems to be a tendency that the isotropic chemical shift decreases with decreasing electronegativity of the second neighboring atom. It therefore appears that in crystalline metavanadates there is no simple linear relation between the δ_{iso} and the EN, differing from ortho- and pyrovanadates. This fact probably indicates that not only the electronegativity of the second neighboring metal cations but also the crystallographic influence, such as the structural unit and linkage mode of VO_n polyhedra, predominate the ^{51}V isotropic chemical shift, because V^{5+} ions form

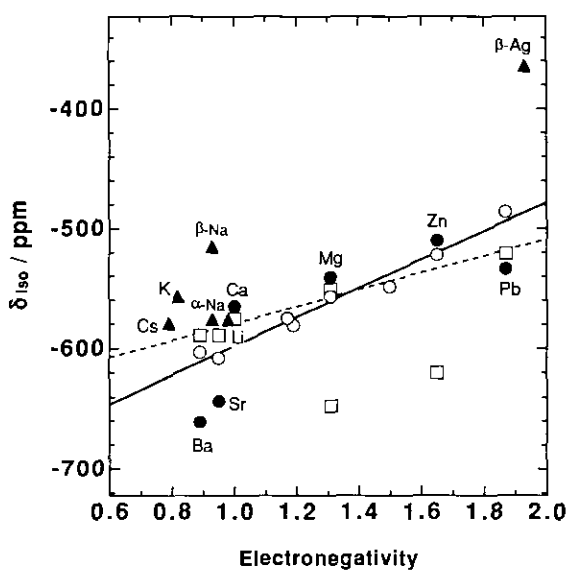

FIG. 6. Plots of the isotropic chemical shift determined from ^{51}V MAS NMR spectra vs Pauling's electronegativity of monovalent and divalent metal (M) for various vanadates. Orthovanadates, ○; pyrovanadates, □; metavanadates, MVO_3, ▲, $M(VO_3)_2$, ●. The solid line and dashed line denote the linear relationships between δ_{iso} and electronegativity for crystalline orthovanadates and pyrovanadates, respectively.

TABLE 3
Isotropic Chemical Shifts Determined by ^{51}V MAS NMR at 9.4 T and Shift Tensors δ_1, δ_2, and δ_3, Chemical Shift Anisotropy, $\Delta\delta$, and Asymmetry Parameter, η, Determined by ^{51}V Static NMR

Compound	$\delta_{iso(MAS)}$	$\delta_{iso(static)}$	δ_1	δ_2	δ_3	$\Delta\delta$	η	Vanadate group	Ref.
				Divalent metal metavanadate					
$Mg(VO_3)_2$	−541	−550	−352	−431	−867	−476	0.25	$(V_2O_8)_n$ chain	This work
$Ca(VO_3)_2$	−565	−566	−272	−351	−1076	−765	0.15	$(V_2O_8)_n$ chain	This work
$Sr(VO_3)_2$	−643	−644	−523	−577	−833	−283	0.29	—	This work
$Ba(VO_3)_2$	−661	−664	−548	−612	−834	−254	0.38	$(VO_3)_n$ chain	This work
$Zn(VO_3)_2$	−510	−512	−302	−381	−852	−511	0.23	$(V_2O_8)_n$ chain	This work
	−495	−533	−270[a]	−410[a]	−920[a]	−580	0.36		(3)
$Pb(VO_3)_2$	−534	−532	−272	−342	−982	−675	0.16	$(V_2O_8)_n$ chain	This work
	−533	−543	−310[a]	−320[a]	−1000[a]	−685	0.02		(3)
				Monovalent metal metavanadate					
$LiVO_3$	−576	−575	−402	−532	−792	−325	0.60	$(VO_3)_n$ chain	This work
		−577.1	−394	−544	−794	−325	0.69		(4)
α-$NaVO_3$	−576	−576	−372	−522	−835	−388	0.58	$(VO_3)_n$ chain	This work
	−576	−577	−360[a]	−530[a]	−840[a]	−395	0.65		(3)
		−578.2	−364	−524	−824	−380	0.65		(4)
β-$NaVO_3$	−515	−525	−252	−252	−1072	−820	0	$(V_2O_8)_n$ chain	This work
		−516.4	−264	−264	−1024	−760	0		(4)
KVO_3	−557	−540	−300	−479	−842	−453	0.59	$(VO_3)_n$ chain	This work
	−553	−557	−300[a]	−500[a]	−870[a]	−470	0.64		(3)
		−557.7	−304	−494	−854	−455	0.64		(4)
$CsVO_3$	−579	−566	−335	−512	−851	−428	0.62	$(VO_3)_n$ chain	This work
		−582.6	−344	−524	−874	−440	0.62		(4)
β-$AgVO_3$	−364	−365	−202	−285	−609	−366	0.34	—	
NH_4VO_3	−570	−570	−383	−522	−804	−352	0.59	$(VO_3)_n$ chain	This work
	−570	−577	−370[a]	−530[a]	−830[a]	−380	0.63		(3)
		−571.5	−374	−524	−814	−365	0.62		(4)
V_2O_5	−614	−613	−305	−305	−1128	−923	0	$(V_2O_8)_n$ chain	This work
	−609	−603	−280[a]	−280[a]	−1250[a]	−970	0		(3)

[a] The chemical shift tensors at 7.05 T. All the values except η have a unit of ppm. The experimental errors of $\delta_{iso(MAS)}$ in this work are ±0.5 ppm.

VO_4 tetrahedra or VO_5 trigonal bipyramids depending on the kinds of the second neighboring cations. This will be discussed later in more detail.

In Fig. 7 the isotropic chemical shifts determined by ^{51}V MAS NMR are plotted against the average V–O bond length together with the data of ortho- and pyrovanadates studied previously (1) for comparison. These plots fall into two groups according to the average V–O bond length. In each group the isotropic chemical shift increases almost linearly with increasing average V–O bond length without respect to monovalent and divalent metal metavanadates. The first group includes ortho-, pyro-, and monovalent metal metavanadates, all of which are constituted of VO_4 tetrahedra. The second group contains monovalent and divalent metal metavanadates, which are constituted of VO_5 trigonal bipyramids except $Ba(VO_3)_2$. This result clearly indicates that if the structural units are the same, the ^{51}V isotropic chemical shifts decrease almost linearly with decreasing average V–O bond length independent of the polymerization degree and the linkage mode of VO_n polyhedra.

The isotropic chemical shifts, δ_{iso}, of the divalent metal metavanadates range from −510 to −661 ppm as known from Table 3. It is interesting to note that most of them overlap with those of the divalent metal orthovanadates ranging from −486 to −608 ppm (I), although the VO_n polyhedron of metavanadates have a much lower symmetry than those of orthovanadates, as shown in Fig. 1. This may indicate the contribution of the V=O double bond character to δ_{iso}, which increases in the order $Zn(VO_3)_2 < Mg(VO_3)_2 < Pb(VO_3)_2 < Ca(VO_3)_2$ as the symmetry of the VO_5 trigonal bipyramid reduces.

The isotropic chemical shifts of crystalline $Sr(VO_3)_2$ and $Ba(VO_3)_2$ are much smaller than those of other metavanadates, although crystalline $Ba(VO_3)_2$ consists of VO_4 tetrahedra and the average V–O bond length is as large as 1.78–1.79 Å compared with other vanadates containing VO_4 tetrahedral units only. According to Table 2, the V–O–V bond angle may be a major structural parameter causing such a remarkable difference in the ^{51}V shielding, since the V–O–V bond angle reflects the nature of hybrid orbitals of V–O bonds (1); the degree of *s* hybridization

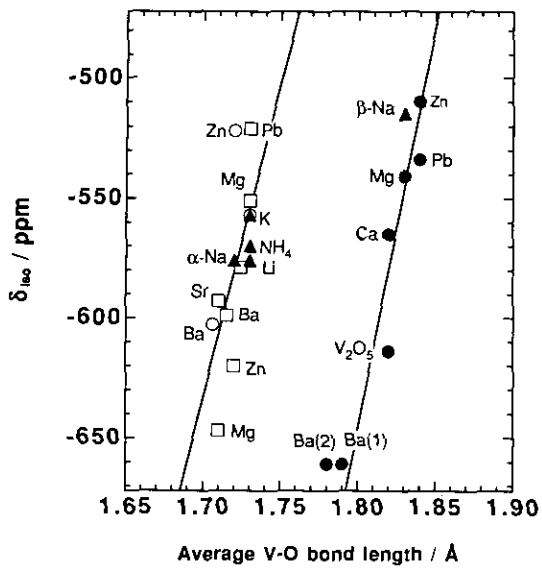

FIG. 7. Plots of the isotropic chemical shift determined from ^{51}V VAS NMR spectra vs the average V–O bond length for various vanadates. Orthovanadates, ○; pyrovanadates, □; metavanadates, MVO_3, ▲, $M(VO_3)_2$, ●.

of the oxygen bond orbitals increases with increasing V–O–V bond angle. Therefore, considerably large V–O–V bond angles, 160° and 156°, of $Ba(VO_3)_2$ may cause the low-frequency shift of ^{51}V in a similar manner to pyrovanadates with a staggered configuration (1).

The ^{51}V Chemical Shift Anisotropy and Asymmetry Parameter

The ^{51}V static NMR lineshapes of the metavanadates are asymmetrical and broad as seen from Figs. 2 and 4. The chemical shift anisotropy, $|\Delta\delta|$, which describes the orientation dependence of the three-dimensional shielding of the ^{51}V nucleus, should be related to the asymmetrical distribution of electron density around the nucleus, which in turn reflects the local environment of vanadium atoms in crystalline vanadates. Figures 8a and 8b represent the plots of the $|\Delta\delta|$ determined by ^{51}V static NMR against Δd_n and the Δa_n, respectively. For comparison, the data of ortho- and pyrovanadates studied previously (1) are also shown by open circles and open squares, respectively. These plots show that the chemical shift anisotropy, $|\Delta\delta|$, increases with increasing Δd_n and Δa_n in metavanadates, indicating that the chemical shift anisotropies are correlated with the structural distortion of a VO_n polyhedron which increases with the coordination number of a vanadium atom and the polymerization degree. That is, $|\Delta\delta|$ seems to be larger in the VO_5 trigonal bipyramids than in the VO_4 tetrahedra and to increase in the order ortho- < pyro- < metavanadates as the polymerization degree increases.

It is seen from Table 3 that for metavanadates consisting of $(VO_3)_n$ single chains the $|\Delta\delta|$ ranges from 254 to 453 ppm and the η from 0.29 to 0.62, and for V_2O_5 and metavanadates consisting of $(V_2O_8)_n$ zigzag double chains $|\Delta\delta|$ ranges from 476 to 923 ppm and the η from 0 to 0.25. This suggests that the values of both $|\Delta\delta|$ and η depend on the vanadate groups or structural unit. In order to examine this relation, the asymmetry parameter, η, is plotted against the chemical shift anisotropy, $|\Delta\delta|$, in Fig. 9 not only for metavanadates but also for ortho- and pyrovanadates previously studied (1). For better understanding, the areas, where the same vanadate groups (see Table 3) are present, are shown in the figure.

The divalent orthovanadates consisting of VO_4^{3-} groups are characterized by a small $|\Delta\delta|$ value within 80 ppm and a very large distribution of η value. The divalent pyrovanadates consisting of $V_2O_7^{4-}$ groups have also a relatively small $|\Delta\delta|$ value from 90 to 180 ppm. Accordingly, it can be said that the ortho- and pyrovanadates are discriminated based on the ^{51}V chemical shift anisotropy.

On the other hand, the metavanadates which contain $(V_2O_8)_n$ zigzag chains consisting of VO_5 trigonal bipyramids exhibit appreciably large $|\Delta\delta|$ over 476 ppm and small $\eta < 0.25$. The monovalent cation metavanadates with $(VO_3)_n$ chains consisting of only VO_4 tetrahedra compose the very restricted region both in $|\Delta\delta|$ and in η between the metavanadates containing $(V_2O_8)_n$ zigzag chains and the pyrovanadates. It is interesting to point out that the range of the chemical shift anisotropy and the asymmetry parameters of metavanadates are much wider than those of ortho- and pyrovanadates. It is therefore possible to predict the structural unit and moreover the polymerization degree, i.e., ortho-, pyro-, and metavanadates, based on the present correlation between $|\Delta\delta|$ and η. In particular, this relationship is useful for examining the structure of unknown crystalline vanadates and vanadate glasses (20).

Correlation between the ^{51}V NMR Parameters and the Crystal Structure

The crystal structure of α-$NaVO_3$ (8) is schematically shown in Fig. 10a, which is constituted of $(VO_3)_n$ single chains. Other monovalent metal metavanadates, such as $LiVO_3$, KVO_3, $CsVO_3$, and NH_4VO_3, except for β-$NaVO_3$ and β-$AgVO_3$, also have a similar structure. The structural similarity between these metavanadates is understandable on the basis of the experimental fact that the asymmetry parameters of these monovalent metal metavanadates are almost the same (see Table 3 and Fig. 10).

The crystal structure of β-$NaVO_3$ (9) is schematically shown in Fig. 10b, which is constituted of $(V_2O_8)_n$ double chains, i.e., edge-shared VO_5 trigonal bipyramids. The

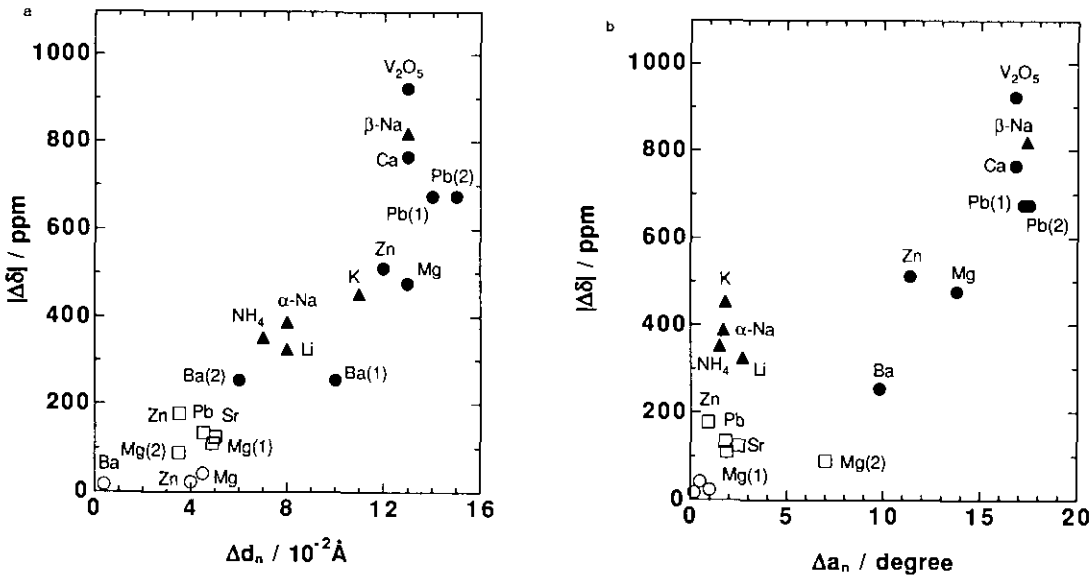

FIG. 8. (a) Plots of $|\Delta\delta|$ vs Δd_n. Orthovanadates, ○; pyrovanadates, □; metavanadates, MVO_3, ▲, $M(VO_3)_2$, ●. (b) Plots of $|\Delta\delta|$ vs Δa_n. Orthovanadates, ○; pyrovanadates, □; metavanadates, MVO_3, ▲, $M(VO_3)_2$, ●.

crystal structure of $Mg(VO_3)_2$ (11) shown in Fig. 10c is also constituted of $(V_2O_8)_n$ double chains. Other divalent metal metavanadates, such as $Ca(VO_3)_2$, $Zn(VO_3)_2$, and $Pb(VO_3)_2$, also have a similar structure to $Mg(VO_3)_2$. The structural similarity of those metavanadates is consistent with chemical shift anisotropies, $|\Delta\delta| > 476$ ppm, and asymmetry parameters, $\eta < 0.25$, as seen from Table 3 and Fig. 9.

The crystal structure of V_2O_5 (15) is shown in Fig. 10d, in which the edge-shared VO_5 trigonal bipyramids compose a layer structure. The large structural anisotropy and highly distorted VO_5 trigonal bipyramid cause the largest $|\Delta\delta|$. The smallest $\eta(=0)$, i.e., the high axial symmetry, is primarily due to the presence of the axial V=O bond.

It is seen from Fig. 9 that the chemical shift anisotropy, $|\Delta\delta|$, of β-$AgVO_3$ is placed on the borderline between the $(VO_3)_n$ single chain and the $(V_2O_8)_n$ double chains. The $|\Delta\delta|$ of β-$AgVO_3$ takes a value between $LiVO_3$ and KVO_3, but the asymmetry parameter, η, is similar to that of $Mg(VO_3)_2$. In the infrared spectrum of β-$AgVO_3$, which is not shown here, the most intense absorption band was observed at 915 cm^{-1}. Botto *et al.* (21) assigned this absorption band to the antisymmetric stretching vibrations of VO_4 tetrahedra in alkali metal metavanadates. Accordingly the crystal structure of β-$AgVO_3$ may be constituted of $(VO_3)_n$ single chains.

It is also seen from Fig. 9 that the $|\Delta\delta|$ of $Sr(VO_3)_2$ and $Ba(VO_3)_2$ are also placed on the borderline between $V_2O_7^{4-}$ and $(VO_3)_n^{n-}$. The crystal structure of $Ba(VO_3)_2$ crystal is schematically shown in Fig. 11 (14), in which the vanadate ions, $(VO_3)_n^{n-}$, contain two structurally different types, a staggered and an eclipsed configuration. The first type is composed of two crystallographically equivalent vanadium sites (site 1), of which the average twist angle about the V–V axis is nearly 52°. The second type is composed of two crystallographically inequivalent vanadium sites, site 1 and site 2, of which the average

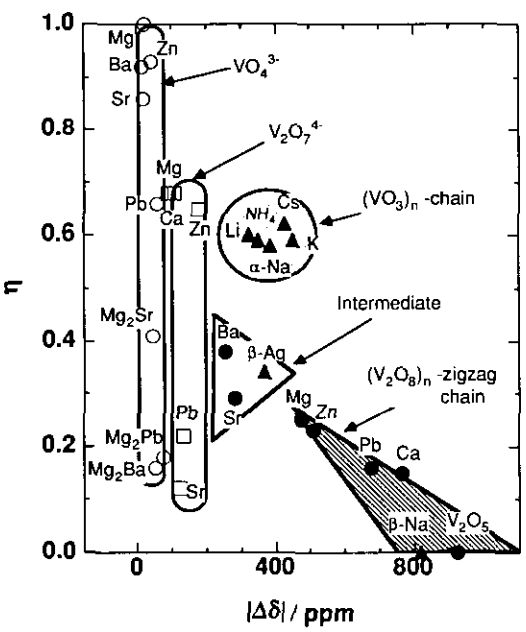

FIG. 9. Plots of η vs $|\Delta\delta|$. Orthovanadates, ○; pyrovanadates, □; metavanadates, MVO_3, ▲, $M(VO_3)_2$, ●.

twist angle about the V–V axis is nearly 11°. Therefore, those two types correspond to pyrovanadate groups with a thortveitite- and a dichromate-type configuration, respectively (1). The chemical shift anisotropies on the borderline of $Sr(VO_3)_2$ and $Ba(VO_3)_2$ are interpreted as being due to the similarity of local configuration between $Ba(VO_3)_2$ and pyrovanadates.

CONCLUSION

^{51}V static and magic-angle spinning (MAS) NMR spectra of crystalline monovalent metal metavanadates $LiVO_3$, α- and β-$NaVO_3$, KVO_3, $CsVO_3$, β-$AgVO_3$, and NH_4VO_3 and divalent metal metavanadates $Mg(VO_3)_2$, $Ca(VO_3)_2$, $Sr(VO_3)_2$, $Ba(VO_3)_2$, $Zn(VO_3)_2$, and $Pb(VO_3)_2$ were measured. The local structure around V^{5+} was discussed on the basis of the relationships between the chemical shift anisotropy, $|\Delta\delta|$, and the asymmetry parameter, η, and the crystallographic parameters together with the results obtained previously for ortho- and pyrovanadates. The following conclusions were drawn.

(1) Very roughly the ^{51}V isotropic chemical shifts tend to decrease as the electronegativity of the second neighboring metal atom decreases, but the relationship is not linear, differing from those for ortho- and pyrovanadates.

(2) As far as the structural units are the same, the ^{51}V isotropic chemical shifts decrease almost linearly with decreasing average V–O bond length, independent of the polymerization degree and linkage mode of the VO_n polyhedra.

(3) The chemical shift anisotropy, $|\Delta\delta|$, increases with the polymerization degree and the degree of the structural distortion of the VO_n polyhedron.

(4) It is found possible to predict the structural unit and the polymerization degree on the basis of the relationship between $|\Delta\delta|$ and η.

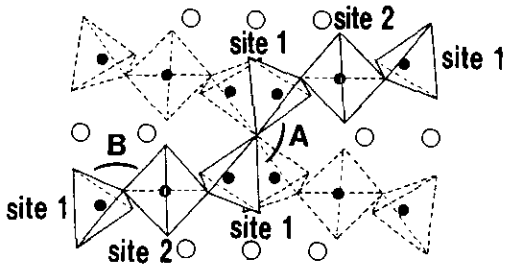

FIG. 11. The arrangement of anions in the crystal structure of $Ba(VO_3)_2$. The open circles and the closed circles represent second neighboring cations (Ba) and vanadium atoms, respectively. (A) staggered configuration (site 1–site 1), B: eclipsed configuration (site 1–site 2) (14).

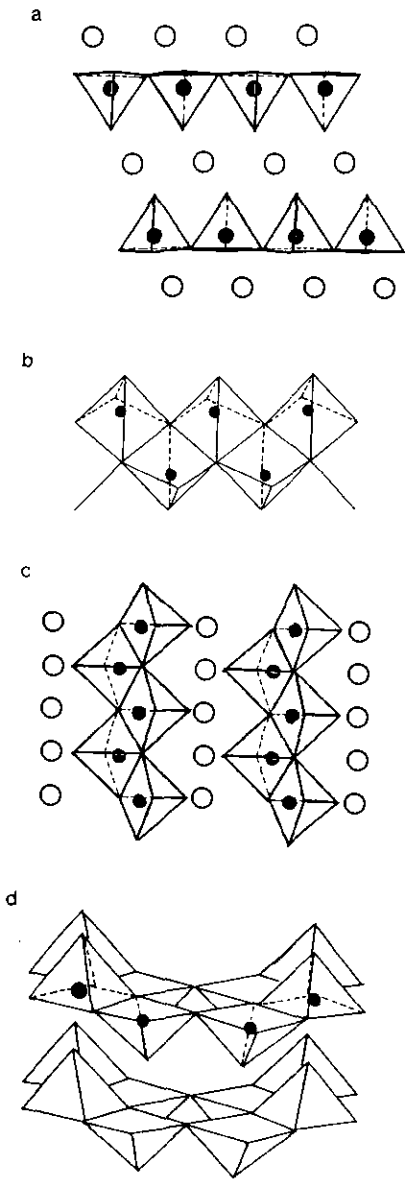

FIG. 10. The arrangement of anions in the crystal structure. The open circles and the closed circles represent second neighboring cations and vanadium atoms, respectively. (a) α-$NaVO_3$, (b) β-$NaVO_3$, (c) $Mg(VO_3)_2$, (d) V_2O_5.

ACKNOWLEDGMENTS

The authors thank Professor F. Horii and Mrs. K. Omine of Kyoto University for their helpful advice and assistance in the NMR measurements. This work was supported by Grant-in-Aid 02403016 for Scientific Research from the Ministry of Education, Science, and Culture, Japan.

REFERENCES

1. S. Hayakawa, T. Yoko, and S. Sakka, *Bull. Chem. Soc. Jpn.* **66,** 3393 (1993).
2. V. M. Mastikhin and O. B. Lapina, *React. Kinet. Catal. Lett.* **24,** 119 (1984).

3. H. Eckert and I. E. Wachs, *J. Phys. Chem.* **93,** 6796 (1989).
4. S. Hayashi and K. Hayamizu, *Bull. Chem. Soc. Jpn.* **63,** 691 (1990).
5. E. Oldfield, R. A. Kinsey, B. Montez, T. Ray, and K. A. Smith, *J. Chem. Soc. Chem. Commun.*, 254 (1982).
6. N. Bloembergen and T. J. Rowland, *Phys. Rev.* **97**(6), 1679 (1955).
7. K. A. Smith, R. J. Kirkpatrick, E. Oldfield, and D. M. Henderson, *Am. Mineral.* **68,** 1206 (1983).
8. F. Marumo, M. Isobe, and S. Iwai, *Acta Crystallogr. Sect. B* **30,** 1628 (1974).
9. K. Kato and E. Takayama, *Acta Crystallogr. Sect. B* **40,** 102 (1984).
10. H. T. Evans, Jr., *Z. Krystllogr.* **Bd-114s,** 257 (1960).
11. H. N. Ng and C. Calvo, *Can. J. Chem.* **50,** 3619 (1972).
12. G. Perez, B. Frit, J. C. Bouloux, and J. Gary, *Compt. Rend.*, **270,** 952 (1970).
13. J. Angenault and A. Rimsky, *C. R. Seances Acad. Sci. Ser. C* **267C,** 227 (1968).
14. S. Launary and J. Thoret, *C. R. Acad. Sci. Paris* **277,** 541 (1973).
15. A. Bystrom, K. A. Wilhelmi, and O. Brotzen, *Acta Chem. Scand.* **4,** 1119 (1950).
16. B. D. Jordan and C. Calvo, *Can. J. Chem.* **52,** 2701 (1974).
17. R. Gopal and C. Calvo, *Can. J. Chem.* **49,** 3056 (1971).
18. P. Fleury and R. Koiilmuller, *C. R. Acad. Sci. Paris* **262,** 475 (1966).
19. R. D. Shannon and C. Calvo, *Can. J. Chem.* **51,** 265 (1973).
20. S. Hayakawa, T. Yoko, and S. Sakka, *J. Ceram. Soc. Jpn.* **102,** 530 (1994).
21. I. L. Botto, E. J. Baran, and P. J. Aymonino, *Mh. Chem.* **107,** 1127 (1976).
22. C. P. Slichter, *"Principles of Magnetic Resonance,"* 3rd ed., p. 605. Springer-Verlag, Tokyo, 1989.